

1 **Surface renewal performance to independently estimate sensible and latent**
2 **heat fluxes in heterogeneous crop surfaces**

3 K. Suvočarev^a, T.M. Shapland^b, R.L. Snyder^c, A. Martínez-Cob^a

4 ^a Dept. of Soil and Water, Estación Experimental Aula Dei (EEAD), CSIC, Avda. Montañana 1005,
5 50059 Zaragoza, Spain, E-mail: suvocarev@eead.csic.es (K. Suvočarev), macoan@eead.csic.es (A.
6 Martínez-Cob)

7 ^b Department of Viticulture and Enology, University of California, Davis, CA 95616, USA, E-mail:
8 tmshapland@ucdavis.edu

9 ^c Department of Land, Air and Water Resources, University of California, Davis, CA 95616, USA, E-
10 mail: rlsnyder@ucdavis.edu

11

12 **Abstract**

13 Surface renewal (SR) analysis is an interesting alternative to eddy covariance (EC)
14 flux measurements. We have applied two recent SR approaches, with different
15 theoretical background, that from Castellví (2004), SR_{Cas} , and that from Shapland et
16 al. (2012a, 2012b), SR_{Shap} . We have applied both models for sensible (H) and latent
17 (LE) heat flux estimation over heterogeneous crop surfaces. For this, EC
18 equipments, including a sonic anemometer CSAT3 and a krypton hygrometer KH20,
19 were located in two zones of drip irrigated orchards of late and early maturing
20 peaches. The measurement period was June to September 2009. The SR_{Cas} is
21 based on similarity concepts for independent estimation of the calibration factor (α),
22 which varies with respect to the atmospheric stability. The SR_{Shap} is based on
23 analysis of different ramp-dimensions, separating the ones that are flux-bearing from
24 the others that are isotropic. According to the results obtained here, there was a high

1 agreement between the 30-min turbulent fluxes independently derived by EC and
2 SR_{Cas} . The SR_{Shap} agreement with EC was slightly lower. Estimation of fluxes
3 determined by SR_{Cas} resulted in higher values (around 11% for LE) with respect to
4 EC, similarly to previously published works over homogeneous canopies. In terms of
5 evapotranspiration, the root mean square error (RMSE) between EC and SR was
6 only 0.07 mm h^{-1} (for SR_{Cas}) and 0.11 mm h^{-1} (for SR_{Shap}) for both measuring spots.
7 According to the energy balance closure, the SR_{Cas} method was as reliable as the
8 EC in estimating the turbulent fluxes related to irrigated agriculture and watershed
9 distribution management, even when applied in heterogeneous cropping systems.

10 *Keywords:* Evapotranspiration, Eddy covariance, Surface renewal, Peach orchard,
11 Energy balance

12

13 **1. Introduction**

14 Precision in sensible (H) and latent heat (LE) flux estimation is important due to their
15 great contribution to precipitation, plant growth, and the amount and locations of
16 surface water runoff. Water use for irrigation purposes is the most important demand
17 to be considered in watershed management. Irrigated agriculture should rely on
18 evapotranspiration (ET) measurements. Together with increasing needs for more
19 arable land and less water use per crop product, there has been a notable
20 improvement in instrumentation, methods and approaches to estimate ET. In order to
21 spread scientifically approved techniques into commercial practice, simpler
22 approaches are preferred. Furthermore, in the absence of possibilities to apply direct
23 measurements of turbulent fluxes such as eddy covariance (EC) or lysimeter

1 measurements of ET losses, surface renewal (SR) (Paw U et al., 1995) has been
2 proposed as a reliable alternative ET estimation method.

3 The energy balance closure is used as a standard procedure to independently
4 evaluate scalar flux estimates derived by micrometeorological methods (Wilson et al.,
5 2002). Where closure is not achieved, flux measurements need to be interpreted to
6 account for inconsistency with conservation principles (Kustas et al., 1999). Several
7 reasons for the lack of closure of the surface energy budget in EC measurements
8 have been discussed by Mahrt (1998): (1) lack of coincidence of the source areas
9 (leaves, soil surface) among various flux components measured very near to a
10 surface; (2) flux divergence arising from transport that is not one-dimensional such as
11 insufficient fetch; (3) non-stationarity of the measured time series; (4) turbulent
12 dispersive fluxes arising from organized planetary-boundary-layer circulations that
13 may have preferred locations so that the mean vertical velocities at an instrument
14 location may be systematically different from zero, hence giving rise to a vertical
15 advective flux; and (5) systematic bias in instrumentation (Twine et al., 2000).

16 When using the SR method, some of the uncertainties related to EC instrumentation
17 could be avoided: no orientation limitations, no leveling requirement, no shadowing or
18 instrumentation separation issues, etc. Likewise, despite Castellví (2012) showed
19 that in practice the fetch requirements for SR are similar as for the EC method,
20 Castellví and Snyder (2009a) showed that the SR method can be operated at any
21 height (roughness or inertial sublayer) and thus the SR is less stringent to the fetch
22 requirements when a sonic anemometer is avoided. In other words, the SR
23 equipment is more adjustable to the specific conditions of fetch (Castellví, 2012).
24 Methodologically, SR is based on canopy layer turbulence and the time-space scalar
25 field associated with the dominance of turbulent coherent structures. Numerous

1 authors (Paw U et al. 1995; Snyder et al. 1996; Spano et al. 1997, 2000; Chen et al.
2 1997a, 1997b; Castellvi and Martínez-Cob 2005; Zapata and Martínez-Cob 2001;
3 Zhao et al. 2010) have used a simple version of the SR method based on analyzing
4 ramp-like patterns in the temperature time series to estimate H. It was proved to be
5 applicable in a wide range of natural surfaces. In this case latent heat flux (i.e. ET
6 expressed in energy terms) was obtained as the residue of the energy balance
7 equation. Detailed theory behind the SR analysis basics and early advances are
8 described in previous works by Paw U et al. (1995; 2005); Snyder et al. (1996); and
9 Spano et al. (1997).

10 The main challenge facing the SR method is deriving the calibration factor (α), thus
11 making SR dependent on other direct surface exchange measurements such as EC.
12 According to some important studies in the topic (Paw U et al., 1995; Snyder et al.,
13 1996; Katul et al., 1996; Duce et al., 1998; Castellvi, 2004), α for sensible heat flux
14 depends on the measurement height, stability conditions, canopy architecture and
15 size and design of the wire if thermocouples are used. When it comes to estimating
16 α , different explanations and methods have been proposed in order to derive
17 repeatable procedures to correct the SR flux results. Namely, Paw U et al. (1995)
18 proposed that the need for calibration arises from uneven coherent structure heating.
19 Afterwards, Castellvi (2004) proposed combining SR analysis with similarity theory to
20 auto-calibrate SR, which requires also average wind speed measurements. One
21 study over rice field demonstrated the feasibility of applying the Castellvi (SR_{Cas})
22 principles to independently derive H and LE (Castellvi et al., 2006). Another study
23 over rangeland grass used SR_{Cas} to estimate three scalar fluxes, demonstrating
24 energy flux densities higher than the ones derived by the EC method: 4%, 18% and
25 10% for H, LE and carbon dioxide (F_p) fluxes, respectively (Castellvi et al., 2008).

1 Castellvi et al. (2006, 2008) showed that this SR_{Cas} estimations improved energy
2 balance closure when applied over homogeneous crop surfaces.

3 Recently, Shapland et al. (2012a, 2012b) proposed a SR method (SR_{Shap}) for
4 independent flux estimation by distinguishing the larger turbulent coherent structures
5 responsible for the flux interchange from the smaller non-flux-bearing isotropic
6 turbulence. Shapland et al. (2012b) applied this approach for the H estimation over
7 bare soil, sorghum and teff grass fields. Their approach demonstrated that no
8 calibration was needed under the unstable atmospheric conditions. Under the
9 hypothesis that the smallest scale turbulent structures (Scale One) mix the larger
10 scale coherent structures (Scale Two), which are responsible for direct energy and
11 mass exchange, α values are shown to be about 1.00.

12 To our knowledge, no other results have been reported on the application of the
13 SR_{Cas} or SR_{Shap} approaches for calculating LE over heterogeneous canopies, where
14 the turbulence can be enhanced by the presence of an uneven ground cover and the
15 assumptions behind similarity theory may not be fulfilled. Thus, we have employed
16 both SR_{Cas} and SR_{Shap} analyses in drip-irrigated peach orchards to estimate
17 independently H and LE flux densities over the data collected by EC equipments.
18 An EC installation was set up in each of two different peach orchards with distinct
19 cultivars to provide a dataset to evaluate performance and applicability of the SR_{Cas}
20 and SR_{Shap} methods over such a heterogeneous crop surface when compared to EC
21 values as a reference. The SR_{Cas} calculation requires high frequency temperature
22 measurements and mean horizontal wind speed data. For SR_{Shap} calculation, only
23 high-frequency scalar measurements are needed.

24

2. Material and methods

2.1. Crop, site and instrumentation

Two EC stations were run from 1 June to 30 September 2009 at a commercial orchard La Herradura in Caspe (NE Spain, middle Ebro River Basin) to measure the surface energy balance components in two drip-irrigated peach orchards. The experimental site was characterized by relatively high winds (long-term annual average wind speed at 2 m above ground is 3.1 m s^{-1}) and semiarid climate (long-term annual precipitation and reference evapotranspiration, 315 and 1392 mm, respectively) (Martínez-Cob and Faci, 2010).

The orchard was located next to a meander of the Ebro River, near to where the river forms a lake upstream of the Mequinenza dam (Fig. 1). The topography was rough, with elevation ranging from 120 to 200 m above the mean sea level (Fig. 2). Peaches represented 154 ha out of 227 ha total in the orchard. About 51 and 52 ha were cropped to early and late maturing peaches, respectively (Fig. 1). The remaining crops were cherries and apricots.

The first EC station (ST1) was set in a late peach zone ($41^{\circ}17'40''$ N latitude, $0^{\circ}00'24''$ E longitude), and the second EC station (ST2) was set in an early peach zone ($41^{\circ}18'21''$ N latitude, $0^{\circ}00'26''$ E) (Fig. 1). Both late and early peach zones included several cultivars with similar phenological characteristics. Row orientation was north to south and canopy height was about 2.5 m for both orchards. The tree and row spacing were 3.75 m and 5.75 m for the late peaches, respectively, and 3.0 m and 5.0 m for the early peaches, respectively.

The soil down to 1.2 m depth was characterized by moderate to low average values of readily available water (70 to 110 mm) depending on the stoniness of a particular

1 zone within the orchard (Zapata et al., 2013). Field capacity and wilting point were
2 0.29 and 0.13 to 0.14, respectively. Drip irrigation was applied daily. Two
3 polyethylene irrigation laterals were used to irrigate each row of trees, one lateral at
4 each side of the row. Turbulent (non-pressure compensating) emitters were used
5 with a design discharge of 4 l h^{-1} . Emitters were extruded in the laterals at 1 m
6 intervals. The discharge volume was $24 \text{ l h}^{-1} \text{ tree}^{-1}$ for early peaches and $30 \text{ l h}^{-1} \text{ tree}^{-1}$
7 for late peaches. Table 1 lists the monthly irrigation amounts during the
8 measurement period. Due to their distinct phenological development (Table 2), late
9 peaches received more irrigation water from June to September compared to the
10 early peaches. Pruning and flower and fruit thinning practices were applied
11 seasonally. Herbicides were applied to control weed growth and thus to minimize the
12 presence of understory vegetation between the tree rows.

13 Both micrometeorological stations consisted of a sonic anemometer (Campbell
14 Scientific, CSAT3), a krypton hygrometer (Campbell Scientific, KH20), a net
15 radiometer (Kipp & Zonen, NR-Lite), an air temperature and relative humidity probe
16 (Vaisala, HMP45C), four soil heat flux plates (Hukseflux, HFP01) and two soil
17 temperature sensors (Campbell Scientific, TCAV). Two data loggers (Campbell
18 Scientific, CR3000) were used to monitor these different sensors. All instruments
19 except the soil sensors were placed on the top of a tower, at $z = 6.9 \text{ m}$ above the
20 ground. The sonic anemometers were placed pointing towards the northwest, about
21 315° from north clockwise in late peaches and 308° from north clockwise in early
22 peaches, as this is the most predominant wind direction in the middle Ebro River
23 area (Martínez-Cob et al., 2010). In addition, a previous study of the wind rose
24 recorded at a nearby standard weather station for 2004 to 2008 (June to September)
25 showed also a similar predominant wind direction. The Krypton hygrometers were

1 installed at about 16 cm horizontal distance from the west side of the CSAT3, slightly
2 shifted behind it relative to the prevailing wind direction. The net radiometers were
3 placed oriented towards south. Soil heat flux plates were buried at 0.1 m depth, two
4 in between rows and the other two in the row. Each soil temperature probe had four
5 thermocouples (chromel-constantan), buried into pairs at 0.03 m and 0.06 m depth
6 above each soil heat flux plate.

7 The 10 Hz raw data included wind speed at the x (u) and y (v) horizontal axes and at
8 the z (w) vertical axis, sonic temperature (T_s), and vapor density [Q, recorded as the
9 natural logarithm of the sensor voltage output according to the KH20 krypton
10 hygrometer specifications (Campbell Scientific, 1996)], as well as air temperature (T_a)
11 and relative humidity (RH) recorded from the Vaisala probes. The loggers also
12 recorded 10 Hz values of net radiation (R_n), soil heat flux plate values and soil
13 temperature, and the corresponding 30-min averages were stored. The recorded soil
14 heat flux values were corrected as described by Allen et al. (1996) using the soil
15 temperature records to get soil heat flux in the soil surface layer. Thus, at each 30-
16 min period, the four soil heat flux values obtained were averaged to get a single
17 value of soil heat flux (G).

18 During the experiment planning stage it was necessary to roughly estimate the best
19 position for setting our measurement equipment as we had to take into account the
20 topographic variability and the irregular shape of the orchards (Figs. 1 and 2).
21 Therefore a rough estimation of fetch requirements and the fraction F of scalar fluxes
22 detected from within the fetch were performed. Allen et al. (1996) suggested using
23 the theoretical considerations of boundary layer development to estimate minimum
24 fetch requirements depending on surface roughness as:

$$1 \quad x_f = \left(\frac{30(z-d)}{z_{om}^{0.125}} \right)^{1.14} \quad [1]$$

2 where x_f [m] is the minimum fetch distance required for complete boundary
 3 development, z [m] is the measurement height above the ground, d [m] is zero-plane
 4 displacement and z_{om} [m] is momentum roughness height of the surface ($0.123 \cdot h$).
 5 This equation is valid for near-neutral conditions. Under stable conditions the
 6 exponent 1.14 should be increased, while it should be decreased under unstable
 7 conditions (Allen et al., 1996). Consequently, fetch requirements are shorter in case
 8 of unstable atmospheric conditions than those from Equation [1]. The experimental
 9 orchards were surrounded by the same or similar species of trees, so the boundary
 10 development was not limited by big changes in the surface roughness (Figs. 1 and
 11 2).

12 Once the fetch distance was estimated, the fraction F of the scalar fluxes coming
 13 from within the aimed distance was calculated using the following Equation from
 14 Allen et al. (1996):

$$15 \quad F = \exp \left(\frac{(z-d) \left(1 - \ln \left(\frac{z-d}{z_{om}} \right) \right) - z_{om}}{k^2 x_f \left(1 - \frac{z_{om}}{z-d} \right)} \right) \quad [2]$$

16 where F is a fraction of H or LE density at the measurement height (z) coming from
 17 the fetch distance (x_f). The Equation [2] overestimates F for stable conditions and
 18 underestimates it under unstable conditions.

19 2.2. Micrometeorological methods and data processing

1 Calculations of fluxes were done over data sets that were previously corrected for: 1)
 2 two-dimensional coordinate rotation of the three wind speed components; 2) the lag
 3 between the vertical wind speed and the temperature data; 3) despiking (discarding
 4 values higher or lower than 4 standard deviations from the mean) the virtual
 5 temperature and water vapor concentration data. Additionally, LE fluxes were
 6 corrected for 1) the oxygen concentration as it affects the Krypton hygrometer and 2)
 7 the effect of the density variation due to the heating of air parcel and volume
 8 changes, i.e. the Webb-Pearman-Leuning correction (Webb et al., 1980). Corrected
 9 data were subsequently led through processing for calculating 30-min turbulent
 10 fluxes For EC procedure, the fluxes, H_{EC} and LE_{EC} , were calculated both in $W m^{-2}$:

$$11 \quad H_{EC} = \overline{\rho_a} \overline{C_p} \overline{w'T_s} \quad [3]$$

$$12 \quad LE_{EC} = \frac{\overline{\lambda w'Q'}}{xKw} \quad [4]$$

13 where the overbar and the apostrophe denote 30-min averages and fluctuations
 14 around the mean, respectively; $\overline{\rho_a}$ [$kg m^{-3}$] is mean air density; $\overline{C_p}$ [$J kg^{-1} K$] is the
 15 specific heat of the air; $\overline{w'T_s}$ is the covariance between w [$m s^{-1}$] and T_s [$^{\circ}K$]; $\overline{\lambda}$
 16 [$J g^{-1}$] is the latent heat of vaporization; $\overline{w'Q'}$ is the covariance between w and Q
 17 [$ln(mV)$]; and xKw [$ln(mV) m^3 g^{-1}$] is the factory calibration factor of the krypton
 18 hygrometer (used to obtain water vapor density in terms of $g m^{-3}$). $\overline{\rho_a}$, $\overline{C_p}$ and $\overline{\lambda}$
 19 were the 30-min averages of the 10 Hz values of ρ_a , C_p and λ computed from the raw
 20 data of T_a and RH. This 30-min time frame was used because for that period of time
 21 stationarity conditions in agricultural surfaces are met and SR_{Cas} analysis relies on
 22 the similarity-based relationships determined for half-hour samples (Castellvi and
 23 Snyder, 2010).

1 The SR_{Cas} analysis was performed using the same high frequency data with the
 2 corrections required for EC. By analyzing the scalar time series with multiple orders
 3 of structure functions, as proposed by Van Atta (1977), it is possible to derive the
 4 repetition frequency of coherent structures renewing the surface layer, the amplitude
 5 of the scalar ramps, and the surface exchange estimates (Paw U et al., 1995; Snyder
 6 et al., 1996). Castellvi et al. (2006, 2008) have applied these structure functions from
 7 Van Atta (1977) to determine the ramp amplitude, but used the Chen et al. (1997b)
 8 approach for the ramp duration. Here we have decided to stick to Van Atta (1977)
 9 approach for both the ramp amplitude and duration:

$$10 \quad S^n(j) = \frac{1}{m-j} \sum_{i=1+j}^m (V_i - V_{i-j})^n \quad [5]$$

11 where V_i and V_{i-j} are high-frequency measurements of either air temperature or water
 12 vapor density between two sequential time lags; j is the sample lag interval; m is the
 13 number of data points in the 30-min time period; i is the summation index; and n is
 14 the structure function order. Van Atta (1977) showed that the modeled ramp
 15 amplitude can be obtained by solving for the real roots of the following cubic
 16 equation:

$$17 \quad y = A^3 + pA + q \quad [6]$$

18 where the coefficient for the linear term, p , is determined from the structure functions
 19 as follows:

$$20 \quad p = 10S^2(j) - \frac{S^5(j)}{S^3(j)} \quad [7]$$

21 and the coefficient for the offset term, q , is determined solely by the third order
 22 structure function:

$$23 \quad q = 10S^3(j) \quad [8]$$

1 Finally, the ramp duration can be found as:

$$2 \quad \tau = -\frac{A^3 j}{S^3(j)} \quad [9]$$

3 It is possible to derive the SR_{Cas} scalar fluxes, sensible ($H_{SR_{Cas}}$) and latent heat fluxes
4 ($LE_{SR_{Cas}}$), both in $W m^{-2}$, at measuring height z [m] by using the ramp characteristics,
5 ramp amplitude and ramp duration (Paw U et al. 1995; Castellví et al. 2006).

$$6 \quad H_{SR_{Cas}} = z \overline{\rho_a} \alpha_T \overline{C_p} \frac{A_T}{\tau_T} \quad [10]$$

$$7 \quad LE_{SR_{Cas}} = z \alpha_q \overline{\lambda} \frac{A_q}{\tau_q} \quad [11]$$

8 again, z is 6.9 m in our case; α is the calibration factor; indexes T and q are to
9 distinguish the ramp dimensions for H and LE, respectively.

10 To estimate the non-dimensional α factor, the one-dimensional diffusion equation
11 with SR analysis and similarity concepts were combined into the following equation
12 valid for the scalars being measured within the inertial sublayer (Castellvi, 2004):

$$13 \quad \alpha = \left[\frac{k(z-d)}{\pi z^2} \tau u_* \phi^{-1}(\xi) \right]^{1/2} \quad [12]$$

14 where, $k \sim 0.4$ is the von Kármán's constant; d [m] is the zero-plane displacement;
15 u_* [$m s^{-1}$] is the friction velocity; $\phi(\xi)$ is the stability function for scalar transport; the
16 stability parameter ξ is defined as $(z-d)/L_O$, where L_O [m] is the Obukhov length.
17 Namely, application of stability functions by Castellví (2004) in deriving the H and LE
18 resulted in improved energy balance closure. No scalar exchange was assumed

1 through the top of the air parcel, therefore, vertical and horizontal advection was
2 neglected (Castellví et al., 2006).

3 In the summary of the SR method and its applications by Paw U et al. (2005), it is
4 explained that the SR method applies in both the roughness and inertial sublayer.

5 The equations for α value calculation employed in this work were considered for the
6 measurements made in the inertial sublayer. Following Sellers et al. (1986), the
7 bottom of the inertial sublayer may be estimated as $z^* = h + 2(h - d) \sim 5/3h$ when $d =$
8 $2/3h$. In our case, counting with 2.5 m canopy height, z^* was calculated to be ~ 4.2 m
9 above ground. Although in some cases under unstable conditions the bottom of
10 inertial sublayer was found to be up to 4 times the crop height (Castellví and Snyder,
11 2009b), we believe that our measurements at $z = 6.9$ m were well inside the inertial
12 sublayer for most of the data.

13 The Obukhov length L_O was calculated by:

$$14 \quad L_O = - \frac{\overline{T_s} u_*^3}{k g w' T_s'} \quad [13]$$

15 where friction velocity was calculated as the square root of covariance between
16 rotated vertical and horizontal wind components (Stull, 1988): $u_* = \sqrt{u'w'}$.

17 The stability functions were assumed to be universal for both scalars. They are
18 defined by Foken (2006) and Högström (1988) as:

$$19 \quad \phi(\xi) = \begin{cases} (0.95 + 7.8\xi) & 0 \leq \xi \leq 1 \\ 0.95(1 - 11.6\xi)^{-1/2} & -2 \leq \xi < 0 \end{cases} \quad [14]$$

20 From the invoked assumptions, Equation [12] is valid when measurements are made
21 over homogeneous canopies and stationary conditions apply during the sampling

1 period, which is typically about half an hour, since dominant energy term in the
2 surface energy balance, net radiation, does not change significantly for such a short
3 period of time. It has been shown that the equation worked well in homogeneous
4 short plant canopies. We have applied the same equations on the sparse orchard
5 grove with peach trees to evaluate both H_{SRCas} and LE_{SRCas} estimation.

6 The structure functions from Van Atta (1977) imply that the surface layer exchange
7 for the stationary period of time is represented with repeating number of ramps that
8 are of the same dimension. Shapland et al. (2012a; 2012b) warn that it is important
9 to identify ramps of different dimension to estimate the efficiency of coherent
10 structures in transporting mass and momentum, which is influenced by the detection
11 scheme (Antonia et al., 1983; Gao et al., 1989; Collineau and Brunet 1993). By
12 expanding structure function analysis to identify two ramp scales, the difference
13 between the smallest coherent structure with “intermittent” gradual rise ramp period
14 and the dominant coherent structure characterized by “persistent” gradual rise ramp
15 period is defined (Shapland et al., 2012a; 2012b). The idea is that the method should
16 consider only the ramp scales that are responsible for the surface-layer exchange
17 (Scale Two) and therefore calculate direct fluxes that do not need calibration. The
18 short duration, Scale One ramps are treated as instantaneous events of mixing air to
19 uniform air parcel heating while residing in the canopy that will later be ejected to
20 atmosphere. Shapland et al., (2012a; 2012b) showed that the dominant ramp scale is
21 actually bearing the surface layer exchange, when it is applied over bare ground and
22 short canopies under unstable conditions.

23 The method first uses the Van Atta (1977) procedure to obtain the Scale One ramp
24 amplitude, ramp period and gradual rise period. Next, the Scale One gradual rise
25 period is compared to the Scale One ramp period to classify its magnitude by using

1 the gradual rise duration as the criterion. If it is shorter than the half of the ramp
2 period, the scale of that event is considered intermittent. In that case, time lag is set
3 equal to Scale One gradual rise period in order to filter it out, and Van Atta procedure
4 is further applied to obtain the Scale Two ramp characteristics. Otherwise, for the
5 longer gradual rise periods that occupy the major part of the ramp period, the ramp is
6 considered as persistent. Then, the calculation of the Two Scale ramp characteristics
7 is done by setting the time lags to be half of the Scale One ramp period. In this way,
8 the Scale One is included in calculation procedure and is identified as the bigger –
9 persistent Scale. By using Two Scale ramp characteristics, the expressions for
10 calculating fluxes are similar to the classical surface renewal, but without α , as it is
11 considered to be ~ 1.00 .

$$12 \quad H_{\text{SRShap}} = z \overline{\rho_a C_p} \frac{A_{T2}}{\tau_{T2}} \quad [15]$$

$$13 \quad LE_{\text{SRShap}} = z \bar{\lambda} \frac{A_{q2}}{\tau_{q2}} \quad [16]$$

14 All calculation procedures were performed using R software (R Development Core
15 Team 2012).

16 Micrometeorological stations were mounted in a way that footprint in the prevailing
17 wind direction was within the same peach plots. Because of the topography and the
18 irregular shape of the studied plots, we only analyzed those 30-min periods for which
19 wind was between $\pm 45^\circ$ of the angle to which sonic anemometers were pointing,
20 308° for late and 315° early peaches (Fig. 2).

21 2.3. Data analyses

1 The performance and energy balance closure of the three methods, EC, SR_{Cas} , and
2 SR_{Shap} were evaluated using linear regression analysis and root square mean error,
3 RSME, (e.g. Jamieson et al., 1998). Furthermore, the ratio $D = \Sigma y / \Sigma x$, where Σy were
4 the SR fluxes or, for energy balance closure evaluation, the LE+H fluxes, while Σx
5 were the EC fluxes or, for energy balance closure evaluation, the Rn-G term. D was
6 calculated to easily express under- or over-estimation of the energy balance or
7 simply to compare scalar fluxes derived by the different methods (Castellví and
8 Snyder, 2010).

9

10 **3. Results and discussion**

11 The general meteorological conditions at the two sites are listed in Table 3. Little
12 difference was noticed. Mean monthly air temperatures were higher in July and
13 August. Rainfall was small during the experiment and the most important rain events
14 occurred in September (Table 1). Vapor pressure deficit was higher for the hotter and
15 drier months. This is a windy area with recorded mean monthly wind velocities, for
16 the experimental season, between 1.9 and 2.7 m s⁻¹. The wind roses for the year
17 2009 at ST1 and ST2 showed slightly different wind direction distribution between
18 both micrometeorological sites probably due to difference in the measuring site
19 elevations and therefore ST1 being more exposed to winds; less calm winds were
20 observed at ST1 (21.7%) than at ST2 (26.1%). Predominant wind directions were
21 west or east (ST1) or west or east to southeast (ST2). East to southeast winds were
22 considered as 'bad wind direction data' as discussed previously and its relatively high
23 frequency led to the removal of more data (about half of total data recorded) than

1 expected according to the general wind direction distributions in the middle Ebro river
2 (Martínez-Cob et al., 2010) and the wind rose for the nearby weather station.

3 The SR_{Cas} estimated α values with respect to stability function for four cases (α_T and
4 α_q for both stations, ST1 and ST2) are represented in Fig. 3. Most of the values were
5 found between 0.25 and 1.5; those for unstable conditions were higher (0.5 to 1.5)
6 than those obtained for stable conditions (0.25 to 1.0). The values for unstable
7 conditions had greater variability than those for stable atmospheric conditions, which
8 tend to have more uniform value under very stable conditions ($\alpha < 0.25$). The
9 uniformity for the stable cases may be because both scalar fluxes were low, so the
10 calibration value was lower and it tended to a constant value. It can be assumed that
11 stationary characteristics for the summer nocturnal conditions in this area also
12 contribute to that small variation in α values. As Equation [12] indicates, the α value
13 is directly dependent on the ramp duration and friction velocity and it is inversely
14 proportional to $\phi(\xi)$. Therefore, it was expected to obtain higher and more variable
15 α values for the unstable conditions when more variability is usual for the daytime
16 parameters. When averaged all values for the stable periods during the measuring
17 season, we have got similar values for α_T and α_q at both sites (0.40 – 0.47). For
18 unstable periods similar values were found at each site, 0.70 and 0.72 for α_T and
19 0.53 and 0.56 for α_q . Nevertheless, the implications of α value are still not well
20 understood, especially under the stable atmospheric conditions (Castellvi, 2004).

21 Shapland et al. (2012a) hypothesized that while ramp gradual rise periods of Scale
22 One are much shorter than those of Scale Two, ramp amplitudes of Scales One and
23 Two are approximately the same. Therefore, it is expected that α is less than 1.00
24 when the Scale One is used in calculation procedure and calibration is necessary,

1 which was seen in the classical SR application. Following the new two Scale model,
2 only the flux-bearing Scale Two structure functions are considered and therefore it is
3 expected that calibration is avoided. Shapland et al. (2012b) argued that the method
4 is not performing satisfactory when some of the assumptions behind the method's
5 theory are violated and then calibration might be needed. Namely, the most probable
6 misleading assumption is the existence of only Two Scales of ramps. Besides, in the
7 same paper the authors state that for the intervals during which the Scale One ramp
8 period is more than 0.5 of the Scale Two ramp period the expanded Van Atta (197)
9 procedure is not as effective at resolving the ramp characteristics of Scale Two,
10 making the Scale Two surface renewal H estimations less accurate.

11 According to Equation [1], the minimum fetch requirements for near-neutral
12 conditions in this experiment should be $x_f = 377$ m for complete boundary
13 development. For that distance the estimated fraction of the H and LE fluxes coming
14 from the targeted canopy, according to Equation [2], would be $F = 85\%$. Relaxed
15 fetch requirements have been stated for the SR method. As discussed earlier, it can
16 be used at variable heights with respect to canopy, i.e. inside the roughness or
17 inertial layer (Paw U et al., 1995, Castellvi and Snyder, 2009a). Also, SR sensors can
18 be mounted at a lower heights than EC instruments to allow the footprint to be well
19 inside the area of interest and to maximize the data collection amount and quality.
20 Nevertheless, in this particular work, we believe that the same fetch requirements
21 rules apply for both EC and SR when CSAT3 is used and measurements for both
22 methods are taken at the same level inside the inertial sublayer, which was explained
23 by Castellví (2012).

24 Due to the similarity assumptions in the SR_{Cas} method, the monthly averages of the
25 half-hour values of SR_{Cas} ramp duration (τ) obtained for both H and LE at both sites

1 were compared (Fig. 4). For each particular month, these mean values represent the
2 average evolution of τ along a 24-h period for each month. There was strong
3 agreement found between τ values obtained for both scalar fluxes, H_{SRCas} and
4 LE_{SRCas} , under both stable and unstable conditions. At the ST1, worse agreement in
5 τ for both scalars was obtained for August when some values of τ differed by 100-
6 200 seconds or more. The ST2 datasets for τ had more noise but were also in
7 agreement when the highest peaks are disregarded. The SR theory is based on the
8 contact time of air coherent structure with plant canopy and corresponding dispersive
9 processes of temperature (or other scalar) exchange (Paw U et al., 1995). Under
10 stable atmospheric conditions, a few minutes can be considered the lifespan of a
11 coherent structure (Gao et al., 1989). Thus, when few minutes is the difference
12 between the ramp durations associated with each scalar, the similarity between heat
13 and water vapor transport by the turbulent air flow may not apply. Some of the higher
14 peaks can be considered as noise, although we attempted to filter out data in order to
15 avoid uncertainty introduced by the results obtained under unfavorable conditions
16 with low levels of turbulence. We can see from the Fig. 4 that the disagreement
17 between τ calculated for the H_{SRCas} and LE_{SRCas} may occur during both stable and
18 unstable atmospheric conditions.

19 Relatively poor performance of both SR_{Shap} and SR_{Cas} methods was observed for
20 estimation of H and LE for stable atmospheric conditions (Table 4). Thus, the
21 computed R^2 values for stable ($0 < \zeta < 1$) H data comparisons between EC and
22 surface renewal methods, SR_{Cas} and SR_{Shap} , were relatively low, 0.32 and 0.28 (late
23 peaches) and 0.45 and 0.35 (early peaches), respectively. For the LE data under the
24 same atmospheric conditions, the comparison between EC and SR_{Cas} and SR_{Shap} ,

1 reported higher R^2 values, 0.48 and 0.60 (late peaches) and 0.63 and 0.67 (early
2 peaches), respectively. In terms of the D statistics, the SR methods gave higher
3 values than EC fluxes. $H_{SR_{Cas}}$ were about 39% (late peaches) and 18% (early
4 peaches) higher and $H_{SR_{Shap}}$ were about 96% (late peaches) and 104% (early
5 peaches) higher for stable atmospheric conditions. For $LE_{SR_{Cas}}$ that overestimation
6 was lower, about 11% for both late and early peaches and for $LE_{SR_{Shap}}$ they were
7 around 40% and 31%, respectively.

8 Under unstable atmospheric conditions ($-2 < \zeta < 0$) less overestimation was
9 observed, but still SR analysis resulted in higher D values in almost all cases.
10 Namely, values for $H_{SR_{Cas}}$ were 6 and 9 % higher than H_{EC} and $H_{SR_{Shap}}$ 6 % higher
11 and 4% lower; $LE_{SR_{Cas}}$ were 11 and 12% and $LE_{SR_{Shap}}$ 10 and 11% higher than the
12 LE_{EC} . R^2 under the same conditions was very high for $H_{SR_{Cas}}$ (0.83 and 0.88) and
13 less for $H_{SR_{Shap}}$ (0.66 and 0.60); also for $LE_{SR_{Cas}}$ (0.76 and 0.86) and less for $LE_{SR_{Shap}}$
14 (0.46 and 0.49).

15 When we compared H and LE data between the EC and SR_{Cas} methods for all
16 atmospheric conditions, agreement was very high as the regression slopes were
17 close to 1.0 (but significantly different from 1.0, level of significance of 0.05) and the
18 intercepts and RMSE were small (Table 4). The different statistics used indicate that
19 SR_{Cas} performed better in estimating the H than LE fluxes. There are no clear
20 reasons why SR_{Cas} performed different in estimating H and LE values. We agree with
21 explanations given by Castellvi et al. (2008) that one possible source of error may lie
22 in correction implemented for unaccounted density variations in incompressible flow.
23 Namely, the WPL correction is sensitive to the propagation of errors stemming from
24 scalar covariance estimation. Nevertheless, when calculating SR_{Cas} fluxes without
25 applying WPL, the results only changed by few percent (data not shown).

1 The SR_{Shap} method showed differences in estimating H and LE fluxes but there was
2 not a clear pattern. We believe that in this case, the data gaps were responsible for
3 inconsistency in the statistics. Scale Two surface renewal data were omitted if the
4 values were unreasonable. The unreasonable values likely arise from poor resolution
5 of the Scale Two ramp characteristics, which occurs when the assumptions behind
6 the expanded Van Atta (1977) method described in Shapland et al. (2012a) are
7 violated. Namely, the variability in the number of datasets obtained for stable or
8 unstable atmospheric conditions possibly influences the statistics to give different
9 measures of agreement.

10 Energy balance closure results for stable, unstable and all atmospheric stability
11 conditions for EC, SR_{Cas} and SR_{Shap} are listed in Table 5. As expected for SR_{Cas}
12 better performance is noticed for unstable conditions than for stable conditions. SR_{Cas}
13 analysis resulted in similar or even slightly better energy balance closure than EC,
14 according to the statistical parameters listed. Statistics from Table 5 for all stability
15 conditions for SR_{Shap} performance are indicating that there was high correlation (with
16 R^2 of 0.81 and 0.80 for early and late peaches, respectively) between Rn-G and
17 SR_{Shap} flux results although it was lower than the one observed in EC and SR_{Cas}
18 analysis. RMSEs showed also poorer performance, especially considering the
19 number of data points analyzed. These results for the SR_{Shap} should be taken with
20 caution due to the limited amount of data points yielded.

21 For the case inclusive of all atmospheric stability conditions, the statistics D indicates
22 that only 6% (late peaches) and 2% (early peaches) of energy was underestimated
23 by turbulent fluxes derived by the SR_{Cas} approach on the seasonal level (Table 5).
24 Slightly poorer performance was observed in case of SR_{Shap} approach with 10 and
25 13% of lack of energy balance closure. EC results showed 13% (ST1) and 12%

1 (ST2) of flux lost in energy balance for all data of the season. The lack of the energy
2 balance closure of 12 and 13% is within earlier reported results for EC
3 measurements over different plant canopies (Wilson et al., 2002). The figures of 6
4 and 2% energy imbalance for the SR_{Cas} method are in agreement with previous
5 SR_{Cas} results reported in publications by Castellvi et al. (2006; 2008). Thus, SR_{Cas}
6 and SR_{Shap} results can be considered as reasonably reliable, although SR_{Shap} dataset
7 was limited by the size of the experimental set. The parameter D should be taken
8 cautiously as it might compensate errors for the sums it uses in calculation. Also, it
9 may lead to confusion when the periods under stable atmospheric conditions are
10 evaluated; as the difference $Rn-G$ and the sum $LE+H$ are often different in sign which
11 have resulted in few negative D values (Table 5). The dew formation may also
12 disturb the sign of data as it is followed by negative LE. Other statistical parameters
13 listed in Table 5 are useful for broader comparison between the reference method
14 (EC) and the new methods (SR_{Cas} and SR_{Shap}). For example, the slopes were closer
15 to unity in all cases for SR, but intercepts were slightly worse when energy balance is
16 estimated. Two more considerations should be mentioned. Firstly, the root square
17 mean error, RSME, in H_{EC} comparison for different brands of EC systems obtained in
18 ideal conditions over short, dense and homogeneous vegetation is found to range
19 between $6.1 - 21 \text{ W m}^{-1}$ (Twine et al., 2000; Mauder et al., 2007). Secondly, the lack
20 of sonic anemometer to “sense” mean vertical wind velocities of very small
21 magnitudes (0.001 m s^{-1}) influences EC results to be underestimates of actual fluxes.
22 It is unknown how a non-zero mean vertical velocity may affect the SR method, but it
23 likely has less impact than in the EC method. Namely, a non-zero \bar{w} might cause an
24 underestimate of the actual flux in SR analysis because it assumes that there is no
25 mass or heat loss through the air parcel top, but the mean vertical displacement of

1 the scalar, while the air parcel is connected to the surface is negligible when
2 compared with the air parcel height (~ 6.9 m in our case). The corresponding error is
3 on the order of 10^{-2} , which is within the instrumental measurement error for vertical
4 placement above the ground (Castellví et al., 2008).

5 In this study, SR_{Cas} approach generally performed well under both stable and
6 unstable conditions, given that the energy balance closure and its components were
7 in agreement with the EC results (Fig. 5). SR_{Shap} , have shown similar performance for
8 energy balance closure to EC and SR_{Cas} , according to values for D statistics, under
9 unstable and all stability conditions. R^2 are lower than the ones obtained for EC or
10 SR_{Cas} . There was more scatter in case of the late peaches (ST1) observed for all
11 methods and less scatter in EC results than in SR_{Cas} or SR_{Shap} for both maturing
12 peach types. Energy balance is, in general, overestimated by all methods for low
13 available energy (Rn-G) values (Fig. 5). For higher values of available energy, the
14 turbulent fluxes are, mostly, underestimated. The crossing value between under- and
15 overestimation of available energy, i.e. where estimated fluxes can close the energy
16 balance equation are found around: 1) 50 W m^{-2} (EC-ST1); 2) 100 W m^{-2} (SR_{Cas} -
17 ST1); 3) 100 W m^{-2} (SR_{Shap} -ST1); 4) 0 W m^{-2} (EC-ST2); 5) 20 W m^{-2} (SR_{Cas} -ST2); 6)
18 no overestimation is observed (SR_{Shap} -ST2). Those values are characteristic for the
19 neutral atmospheric conditions in the early morning or the late afternoon. Generally
20 the agreement between H+LE and Rn-G was better for early morning than for late
21 afternoon hours although the flux underestimation was common phenomenon for the
22 micrometeorological methods. Additionally, it was noticed that for great evaporative
23 demand, LE values were very high, but H+LE almost never reached energy balance
24 closure. As a consequence of all the uncertainties that are related to the EC method,

1 the regression analysis resulted in the slopes significantly different from 1.0 and the
2 intercepts significantly different from 0.0 (level of significance equal to 0.05).

3 All the calculated statistics indicators (slope, intercept, R^2 , RMSE and D) of the data
4 quality better performed for the energy balance closure obtained at the ST2 (Table
5 5). Also, there was a higher agreement between EC and SR_{Cas} results for this site
6 (Table 4). For SR_{Shap} R^2 results were not very consistent (Table 4). The conditions for
7 micrometeorological measurements seemed to be more favorable at the station ST2.
8 There are a few possible explanations for this kind of behavior, including the terrain
9 complexity over the surface considered for the measurement footprint. As it can be
10 seen in Fig. 2 the terrain close to ST1 is sloping down from the measurement spot, at
11 150 m height, to the fetch limit, at 130 m height above mean sea level. There is also
12 a hilly zone that is limiting a part of footprint flux contribution at both ST1 and ST2
13 which was the reason to decide to stay only with those periods when the wind
14 direction was between $\pm 45^\circ$ of the CSAT3 orientation angle. In the ST2 case, sloping
15 down is towards the point where the measurements were set, at 120 m above the
16 mean sea level. Gradual rise of the terrain occurs in the direction of the fetch limit, at
17 150 m above the mean sea level. It seems that this change in the terrain leveling can
18 influence the EC method performance and therefore also the SR. Namely, the
19 CSAT3 is sensitive to the complex terrain issues and thus limits the accuracy of the
20 methods depending on such measurements. According to Baldocchi et al. (2000)
21 advection of mass and energy can occur in circumstances when the underlying
22 surface is heterogeneous. The cases where it can be expected more often are sites
23 with different roughness or different source/sink strength transitions such as between
24 forests and crops, vegetation and lakes, and desert and irrigated crops (Rao et al.,
25 1974; Bink, 1996; Sun et al., 1997). Unfortunately we did not have any measurement

1 equipment set that would describe the possibility of advection. Another possible
2 cause of differences between the two sites is the tree plantation design. As it is a
3 heterogeneous crop plantation, the larger distances in tree plantation both between
4 rows and the tree trunks in the row for the ST1 might be of importance. More
5 contribution to the scalar fluxes by the understory vegetation is expected in orchards
6 with more widely spaced trees, further contributing to the surface heterogeneity.

7 Here, we have used the simplified energy balance equation, while F_p was ignored for
8 lack of adequate equipment. Improving the precision in estimating $H+LE+F_p$
9 according to the appropriate method and representative surface with sufficient fetch
10 has a long-term impact on analyzing the watershed management for agricultural use,
11 carbon sequestration, and climate model validations and calibrations (Oncley et al.,
12 2007; Baldocchi et al., 2004). Castellvi et al. (2008) neglected F_p from energy
13 balance equation, stating that estimation of this variable in rangeland grass were
14 negligible ($-14 \text{ W m}^{-2} < F_p < 5 \text{ W m}^{-2}$). However, F_p might explain some part of the
15 flux loss in the sparse, moderately tall canopies.

16 Our results are confirming that there is no need for calibration of SR_{Cas} against
17 another method to obtain accurate LE data (and ET estimates) even in
18 heterogeneous canopies. SR_{Shap} method performed relatively well, with α values
19 close to 1.00 for unstable cases, which proves the importance of distinguishing
20 between different ramp scales. It may be that even larger ramp scales, and not the
21 detected Scale One or Scale Two, are relevant to surface-layer fluxes during stable
22 conditions. If this is the case, more research is needed to develop methods for
23 determining the number of ramp scales in a time series and which scale is important
24 for the flux.

1 Following Castellvi (2004) there are two options for measurement sets to meet the
2 needs for data collection for the presented auto-calibration SR method: 1) to have
3 only high frequency temperature measurements and mean wind velocity; and 2) to
4 have high frequency measurements of both temperature and wind velocity. As we
5 deployed EC equipment, we suffered a great amount of data loss because of the
6 CSAT3 orientation needs, fetch requirements for proper EC operation, and the SR_{Cas}
7 and SR_{Shap} calculation procedures itself; thus we believe that the SR_{Cas} and SR_{Shap}
8 methods did not completely show its potential performance in this work because
9 some of the uncertainties and shortcomings of the EC method should have affected
10 the SR analyses, too. We could expect at least similar results in those experimental
11 layouts where fine-wire thermocouples are used with cup anemometer, thus reducing
12 minimum fetch limits and avoiding some of the above mentioned problems (Castellví,
13 2012). This may lead to more confidence in applying fine-wire thermocouples alone
14 or together with high-frequency measurements of water vapor density when applying
15 SR_{Cas} analysis. In that case cup anemometer would be necessary in deriving some
16 parameters such as Obukhov length and friction velocity. SR_{Shap} method should be
17 validated more to be applied independently for ET estimation.

18

19 **4. Conclusions**

20 When considering all stability conditions together, energy imbalance for SR_{Cas}
21 results, expressed in terms of the statistics D, was quite good, about 2 to 6 %, while
22 the D statistics for the imbalance for SR_{Shap} was similar to EC, about 13 %. Taking
23 into account together the different statistics, D, slope, intercept and RMSE, we can
24 state that SR_{Cas} has shown similar or only slightly better energy balance closures.

1 SR_{Shap} has shown similar tendency like SR_{Cas} but the performance was slightly
2 poorer. It should be tested in future because of the limited number of data points it
3 yielded for our measurement set and for the calculation procedure itself. However it
4 has shown that the same principles apply in the sparse heterogeneous crop as
5 earlier shown in short homogenous or bare soil. It also showed potential application
6 in LE estimation.

7 A good correlation between turbulent fluxes obtained by EC and SR_{Cas} ('all stability
8 periods' and 'unstable periods' cases) was found (with R^2 ranging between 0.82 and
9 1.00). For the same atmospheric conditions, the analysis of turbulent fluxes
10 estimated by EC and SR_{Shap} showed good correlation (with corresponding values
11 ranging between 0.49 and 0.79). Better correlation is observed in H fluxes
12 comparison. Shapland et al. (2012b) published results that show better correlation for
13 unstable than stable cases for H calculation. We have noticed that LE_{SRShap} to LE_{EC}
14 comparison resulted in higher R^2 values for stable than unstable conditions.

15 Some overestimation in fluxes determined by SR_{Cas} was noticed in agreement with
16 earlier published works in homogeneous canopies. Expressing the RMSE values
17 from Table 4 in terms of water depth (ET), the average uncertainty of the SR methods
18 compared to the EC method was very small, around 0.07 mm h^{-1} for SR_{Cas} and
19 around 0.11 mm h^{-1} for SR_{Shap} . These results confirmed the auto-calibration feature
20 of the SR_{Cas} and SR_{Shap} method according to atmospheric stability conditions despite
21 that some lack of similarity for temperature and water vapor exchange is possible
22 under stable atmospheric conditions.

23 In summary we suggest usefulness of the methods SR_{Cas} and SR_{Shap} as interesting
24 alternatives to the EC for the irrigation management in heterogeneous crop for its

1 high performance in statistical comparison and due to demonstrated independency of
2 operation.

3

4 **Acknowledgments**

5 Work funded by the project Consolider CSD2006 – 00067 (Ministerio de
6 Ciencia e Innovación, Spain). Thanks are due to the owners of the commercial
7 orchard, to J.L. Gracia (farm manager), M. Izquierdo, J. Gaudó, J.M. Acín, E.
8 Medina, and C. Merino for technical and field assistance; and to the manuscript
9 reviewers for their useful comments.

10

11 **References**

- 12 Antonia, R.A., Rajagopalan, A., Chambers, A.J., 1983. Conditional sampling of
13 turbulence in the atmospheric surface layer. *J. Clim. Appl. Meteorol.* 22:69–78
- 14 Allen, R.G., Pruitt, W.O., Businger, J.A., Fritschen, L.J., Jensen, M.E., Quinn, F.H.,
15 1996. Evaporation and transpiration. In: Heggen, R.J., Wootton, T.P., Cecilio,
16 C.B., Fowler, L.C., Hui, S.L. (Eds.), *Hydrology Handbook*. 2nd ed. American
17 Society of Civil Engineers, New York, pp. 125–252.
- 18 Baldocchi, D.D., Finnigan J.J., Wilson, K.W. et al., 2000. On measuring net
19 ecosystem carbon exchange in complex terrain over tall vegetation. *Boundary*
20 *Layer Meteorology*, 96, 257-291
- 21 Baldocchi, D.D., Liukang, X., Kiang, N., 2004. How plant functional-type, weather,
22 seasonal drought, and soil physical properties alter water and energy fluxes of an
23 oak-grass savanna and an annual grassland. *Agric. For. Meteorol.* 123, 13-39.

- 1 Bink, N.J., 1996. The Structure of the Atmospheric Surface Layer Subject to Local
2 Advection, Ph.D. Thesis. Agricultural University, Wageningen, The Netherlands
- 3 Campbell Scientific, 1996. Eddy covariance system operator´s manual CA27 and
4 KH20, Revision 9/96. Campbell Scientific, Inc. Logan.
- 5 Castellví, F., 2004. Combining surface renewal analysis and similarity theory: a new
6 approach for estimating sensible heat flux. *Water Resour. Res.* 40, W05201 doi:
7 10.1029/2003WR002677
- 8 Castellví, F., Martínez-Cob, A., 2005. Estimating sensible heat flux using surface
9 renewal analysis and flux variance method: A case study over olive trees at
10 Sastago (NE of Spain). *Water Resour. Res.* 41, W09422, 1-10.
- 11 Castellví, F., Martínez-Cob, A., Pérez-Coveta, O., 2006. Estimating sensible and
12 latent heat fluxes over rice using surface renewal. *Agric. For. Meteorol.* 139, 164-
13 169
- 14 Castellví, F., Snyder, R.L., Baldocchi, D.D., 2008. Surface energy-balance closure
15 over rangeland grass using the eddy covariance method and surface renewal
16 analysis. *Agric. For. Meteorol.* 148, 1147–1160.
- 17 Castellví, F., Snyder, R.L., 2009a. On the performance of surface renewal analysis to
18 estimate sensible heat flux over two growing rice fields under the influence of
19 regional advection. *J. Hydrol.* 375, 546-553
- 20 Castellví, F., Snyder, R.L., 2009b. Sensible heat flux estimates using surface renewal
21 analysis. A study case over peach orchard. *Agric. For. Meteorol.* 149, 1397 – 1402
- 22 Castellví, F. and Snyder, R.L., 2010. A comparison between latent heat fluxes over
23 grass using a weighing lysimeter and surface renewal analysis. *J. Hydrol.* 381,
24 213–220.

- 1 Castellví, F., 2012. Fetch requirements using surface renewal analysis for estimating
2 scalar surface fluxes from measurements in the inertial sublayer. *Agric. For.*
3 *Meteorol.* 152, 233-239
- 4 Chen, W., Novak, M.D., Black, T.A., Lee, X., 1997a. Coherent eddies and
5 temperature structure functions for three contrasting surfaces. Part I: Ramp model
6 with finite micro-front time. *Bound-Lay. Meteorol.* 84, 99-123
- 7 Chen, W., Novak, M.D., Black, T.A., Lee, X., 1997b. Coherent eddies and
8 temperature structure functions for three contrasting surfaces. Part II: Renewal
9 model for sensible heat flux. *Bound. Layer Meteorol.* 84, 125–147.
- 10 Collineau, S., Brunet, Y., 1993. Detection of turbulent coherent motions in a forest
11 canopy. Part II: Time-scales and conditional averages. *Bound. Layer Meteorol.*
12 66:49–73
- 13 Duce, P., Spano, D., Snyder., R.L., 1998. Effect of different fine wire thermocouple
14 design on high frequency temperature measurement. 23rd Conference on
15 Agricultural and Forest Meteorology, Albuquerque, New Mexico, U.S.A.,
16 November 2-6, 1998, pp. 146-147.
- 17 Foken, T., 2006. 50 years of the Monin-Obukhov similarity theory. *Boundary-Layer*
18 *Meteorol.* 119, 431–447.
- 19 Gao, W., Shaw, R.H., Paw U, K.T., 1989. Observation of organized structure in
20 turbulent flow within and above a forest canopy. *Bound. Layer Meteorol.* 47, 349–
21 377.
- 22 Högström, U., 1988. Non-dimensional wind and temperature profiles in the
23 atmospheric surface layer; a re-evaluation. *Bound. Lay. Meteorol.* 42, 55-78

- 1 Jamieson, P.D., Porter, J.R., Goudriaan, J., Ritchie, J.T., van Keulen, H., Stol, W.,
2 1998. A comparison of the models AFRCWHEAT2, CERES-Wheat, Sirius,
3 SUCROS2 and SWHEAT with measurements from wheat grown under drought.
4 *Field Crops Res.* 55, 23–44.
- 5 Katul, G., Hsieh, C., Oren, R., Ellsworth, D., Philips, N., 1996. Latent and sensible
6 heat flux predictions from a uniform pine forest using surface renewal and flux
7 variance methods, *Boundary Layer Meteorol.*, 80, 249– 282.
- 8 Kustas, W.P., Prueger, J.R., Humes, K.S., Starks, P.J., 1999. Estimation of surface
9 heat fluxes at field scale using surface layer versus mixed layer atmospheric
10 variables with radiometric temperature observations. *J. Appl. Meteorol.* 38, 224–
11 238.
- 12 Mahrt, L., 1998. Flux sampling errors for aircraft and towers. *J. Atmos. Oceanic*
13 *Technol.* 15, 416–429.
- 14 Martínez-Cob, A., Faci, J.M., 2010. Evapotranspiration of a hedge-pruned olive
15 orchard in a semiarid area of NE Spain. *Agric. Water Manage.* 97, 410–418.
- 16 Martínez-Cob, A., Zapata, N., Sánchez, I., 2010. Viento y Riego: la variabilidad del
17 viento en Aragón y su influencia en el riego por aspersión. Publication No. 2948.
18 *Series Studies (Geography)*. Institución Fernando el Católico. Zaragoza, Spain.
19 200 pp. [in Spanish]
- 20 Mauder, M., Oncley, S.P., Vogt, R., Weidinger, T., Ribeiro, L., Bernhofer, C., Foken,
21 T., Kosiek, W., De Bruin, H.A.R., Liu, H., 2007. The energy balance experiment
22 EBEX-2000. Part II: Intercomparison of eddy-covariance sensors and post-field
23 data processing methods. *Bound. Layer Meteorol.* 123, 29–54.

- 1 Oncley, S.P., Foken, T., Vogt, R., Kohsiek, W., DeBruin, H.A.R., Bernhofer, C.,
2 Christen, A., Van Gorsen, E., Grantz, D., Feigenwinter, C., Lehner, I., Liebenthal,
3 C., Liu, H., Mauder, M., Pitacco, A., Ribeiro, L., Weidinger, T., 2007. The energy
4 balance experiment EBEX-2000. Part I: overview and energy balance. Bound.
5 Layer Meteorol. 123, 1-28.
- 6 Paw U, K.T., Qiu, J., Su, H.B., Watanabe, T., Brunet, Y., 1995. Surface renewal
7 analysis: a new method to obtain scalar fluxes without velocity data. Agric. For.
8 Meteorol. 74, 119–137.
- 9 Paw U, K.T., Snyder, R.L., Spano, D., Su, H.B., 2005. Surface renewal estimates of
10 scalar exchanges, Micrometeorology in Agricultural Systems, Agron. Monogr., vol.
11 47, pp. 445 – 484, ASA-CSSA-SSSA, Madison, Wisc.
- 12 R Development Core Team 2012. R: A language and environment for statistical
13 computing. R Foundation for Statistical Computing, Vienna, Austria, ISBN-900051-
14 07-0
- 15 Rao, K.S., Wyngaard, J.C., Cote, O.R., 1974. Local Advection of Momentum, Heat,
16 and Moisture in Micrometeorology, Bound. Layer Meteorol. 7, 331–348.
- 17 Shapland, T.M., McElrone, A.J., Snyder, R.L., Paw U, K.T., 2012a. Structure
18 Function Analysis of Two-Scale Scalar Ramps. Part I: Theory and Modelling.
19 Bound. Layer Meteorol. 145, 5-25 DOI 10.1007/s10546-012-9742-5
- 20 Shapland, T.M., McElrone, A.J., Snyder, R.L., Paw U, K.T., 2012b. Structure
21 Function Analysis of Two-Scale Scalar Ramps. Part II: Ramp Characteristics and
22 Surface Renewal Flux Estimation. Bound. Layer Meteorol. 145, 27-44 DOI
23 10.1007/s10546-012-9740-7

- 1 Sellers, P.J., Mintz, Y., Sud, Y.C., Dalcher, A., 1986. A simple biosphere model (SiB)
2 for use within general circulation models, *J. Atmos. Sci.* 43, 505–531.
- 3 Snyder, R.L., Spano, D., Paw U, K.T., 1996. Surface renewal analysis for sensible
4 and latent heat flux density. *Bound. Layer Meteorol.* 77, 249–266
- 5 Spano D, Snyder RL, Duce P, Paw UKT, 1997. Surface renewal analysis for sensible
6 heat flux density using structure functions. *Agric. For. Meteorol.* 86, 259–271
- 7 Spano, D., Snyder, R.L., Duce, P., Paw U, K.T., 2000. Estimating sensible and latent
8 heat flux densities from grapevine canopies using surface renewal. *Agric. For.*
9 *Meteorol.* 104, 171–183.
- 10 Stull, R.B., 1988. *An Introduction to Boundary Layer Meteorology*. Kluwer
11 Academic, 666 pp.
- 12 Sun, J., Lenschow, D. H., Mahrt, L., Crawford, D. L., Davis, K. J.,
13 Oncley, S. P., MacPherson, J. I., Wang, Q., Dobosy, R. J., and Desjardins, R. L.,
14 1997. Lake-Induced Atmospheric Circulations during BOREAS, *J. Geophys. Res.*
15 102, 29155–29166
- 16 Twine, T.E., Kustas, W.P., Norman, J.M., Cook, D.R., Houser, P.R., Meyers, T.P.,
17 Prueger, J.H., Starks, P.J., Wesely, M.L., 2000. Correcting eddy-covariance flux
18 underestimates over a grassland. *Agric. For. Meteorol.* 103 , 279–300.
- 19 Van Atta, C.W., 1977. Effect of coherent structures on structure functions of
20 temperature in the atmospheric boundary layer. *Arch Mech* 29,161–171
- 21 Webb, E.K., Pearman, G.I., Leuning, R., 1980. Correction of Flux Measurements for
22 Density Effects Due to Heat and Water Vapour Transfer. *Quart. J. Roy. Meteorol.*
Soc. 106, 85–100.

- 1 Wilson, K., Goldstein, A., Falge, E., Aubinet, M., Baldocchi, D., Berbigier, P.,
2 Bernhofer, C., Ceulemans, R., Dolman, H., Field, C., Grelle, A., Ibrom, A., Law,
3 B.E., Kowalski, A., Meyers, T., Moncrieff, J., Monson, R., Oechel, W., Tenhunen,
4 J., Valentini, R., Verma, S., 2002. Energy balance closure at FLUXNET sites.
5 113,223–243
- 6 Zapata, N., Martínez-Cob, A., 2001. Estimation of sensible and latent heat flux from
7 natural sparse vegetation surfaces using surface renewal. *J. Hydrol.* 254, 215-228.
- 8 Zapata, N., Nerilli, E., Martínez-Cob, A., Chalghaf, I., Chalghaf, B., Fliman, D.,
9 Playán, E., 2013. Limitations to adopting regulated deficit irrigation in stone fruit
10 orchards: a case study. *Spanish Journal of Agricultural Research.* 11 , 529-546.
- 11 Zhao, X., Liu, Y., Tanaka, H., Hiyama, T., 2010. A comparison of flux variance and
12 surface renewal methods with eddy covariance. *IEEE Journal of Selected Topics*
13 *in Applied Earth Observations and Remote Sensing.*3,345-350 DOI:
14 10.1109/JSTARS.2010.2060473

1

2 Table 1. Monthly irrigation and precipitation amounts during the measurement
3 periods.

Maturing		June	July	August	September	Total
type						
Irrigation	Late	88.8	116.8	87.1	88.6	494.3
(mm)	Early	147.3	94.9	57.0	29.9	442.1
Precipitation (mm)		25.6	24.8	30.4	32.2	113.0

4

1

2 Table 2. Phenology of the studied peach cultivar types.

Maturity type	Blooming	Pit hard	Harvest begins	Harvest ends	Leaf fall
Late	13-mar	14-jun	13-sep	06-oct	15-nov
Early	03-mar	06-may	18-jun	27-jun	30-oct

3

4

1

2 Table 3. General mean monthly meteorological conditions within the experimental period
3 recorded at the two measurement spots, late maturing (ST1) and early maturing (ST2)
4 peaches: T, air temperature; VPD, air vapor pressure deficit; WV, wind velocity.

	T		VPD		WV	
	[°C]		[kPa]		[m s ⁻¹]	
	ST1	ST2	ST1	ST2	ST1	ST2
June	24.1	24.2	1.2	1.2	2.3	2.1
July	25.8	26.0	1.2	1.3	2.7	2.5
August	25.9	26.3	1.1	1.1	2.0	2.0
September	21.2	21.5	0.7	0.7	2.0	1.9

5

1

2 Table 4. Comparison between eddy covariance sensible and latent heat fluxes (H_{EC} and LE_{EC}) and the
3 corresponding fluxes derived by the surface renewal method in two peach maturing types: a) following
4 Castellvi et al., (2006, 2008) (H_{SRCas} and LE_{SRCas}); b) following Shapland et al. (2012a, b) (H_{SRShap} and
5 LE_{SRShap}). H_{EC} and LE_{EC} were considered as independent variable (x) for regression analysis. b_1 ,
6 regression slope; b_0 , regression intercept; R^2 , coefficient of determination; RMSE, root mean square
7 error; D, ratio of total sums ($\Sigma y/\Sigma x$); N, number of values available; Var., variable.

Peach	Var. x	Var. y	Stability	b_1	b_0	R^2	RMSE	D	N
					$W m^{-2}$		$W m^{-2}$		
Late	H_{EC}	H_{SRCas}	Stable	0.76	-13.67	0.32	19.93	1.39	984
			Unstable	1.04	1.16	0.83	25.85	1.06	1062
			All	0.93	0.04	1.00	23.19	0.93	2046
	H_{EC}	H_{SRShap}	Stable	1.02	-18.44	0.28	40.07	1.96	412
			Unstable	1.16	-8.26	0.66	45.96	1.06	436
			All	1.20	-12.97	0.79	42.27	0.80	848
	LE_{EC}	LE_{SRCas}	Stable	0.61	17.67	0.48	45.60	1.11	958
			Unstable	0.94	29.35	0.76	51.47	1.11	1047
			All	0.96	16.10	0.82	48.75	1.11	2005
	LE_{EC}	LE_{SRShap}	Stable	1.26	4.58	0.60	53.05	1.40	636
			Unstable	0.93	31.21	0.46	93.32	1.10	418
			All	1.04	12.06	0.68	71.78	1.17	1054
Early	H_{EC}	H_{SRCas}	Stable	0.99	-5.28	0.45	19.75	1.18	1016
			Unstable	1.07	1.91	0.88	21.70	1.09	789
			All	1.10	-1.47	0.92	20.62	1.01	1805
	H_{EC}	H_{SRShap}	Stable	1.67	-10.78	0.35	49.88	2.04	262
			Unstable	0.99	-1.85	0.60	39.15	0.96	334
			All	1.19	-20.88	0.79	44.19	0.53	596
	LE_{EC}	LE_{SRCas}	Stable	0.90	7.47	0.63	43.00	1.11	964
			Unstable	1.04	16.66	0.86	49.34	1.12	717
			All	1.05	6.70	0.88	45.81	1.12	1681
	LE_{EC}	LE_{SRShap}	Stable	1.19	4.19	0.67	44.24	1.31	522
			Unstable	1.08	6.44	0.49	111.74	1.11	284
			All	1.09	6.30	0.73	75.28	1.16	806

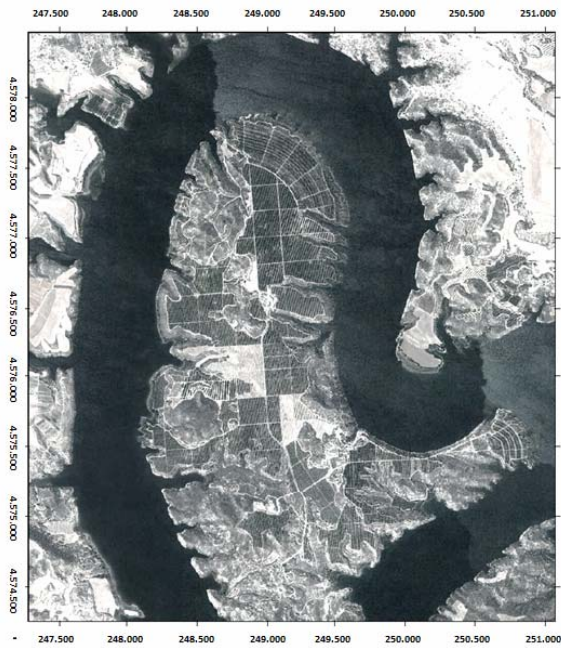
1
2
3
4
5
6
7
8
9

Table 5. Energy balance closure performance for the a) eddy covariance (subscripts 'EC'), b) surface renewal following Castellvi et al., (2006, 2008) (subscripts 'SRCas') and c) surface renewal following Shapland et al. (2012a, b) (subscripts 'SRShap') estimated fluxes at two different peach maturing type spots. Available energy (Rn-G) was considered as independent variable (x) to be compared to the sum of turbulent fluxes (H+LE) variable (y) in regression analysis. b_1 , regression slope; b_0 , regression intercept; R^2 , coefficient of determination; RMSE, root mean square error; D, ratio of total sums ($\Sigma y/\Sigma x$); N, number of values available; Var., variable.

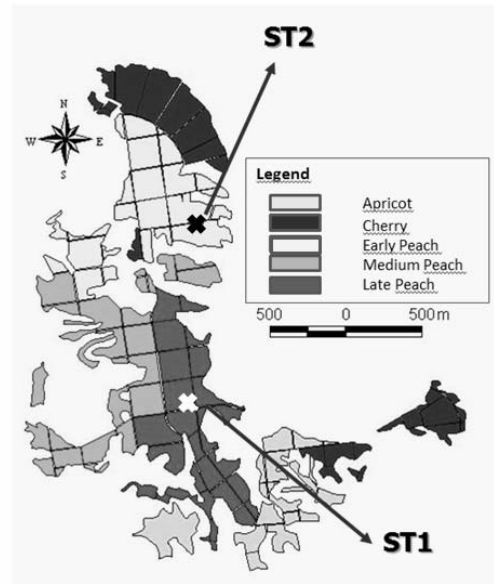
Peach	Var. x	Var. y	Stability	b_1	b_0 W m ⁻²	R^2	RMSE W m ⁻²	D	N
Late	(Rn-G) _{EC}	(H+LE) _{EC}	Stable	0.66	18.94	0.50	53.65	-1.31	983
			Unstable	0.74	19.63	0.76	95.74	0.81	1059
			All	0.74	20.33	0.87	78.35	0.87	2042
	(Rn-G) _{SRCas}	(H+LE) _{SRCas}	Stable	0.61	14.77	0.50	51.17	-0.94	957
			Unstable	0.72	51.80	0.61	104.05	0.89	1046
			All	0.78	24.27	0.82	83.09	0.94	2003
	(Rn-G) _{SRShap}	(H+LE) _{SRShap}	Stable	1.07	11.77	0.71	53.16	-2.85	326
			Unstable	0.84	4.30	0.51	121.09	0.86	269
			All	0.85	7.94	0.80	90.91	0.90	595
Early	(Rn-G) _{EC}	(H+LE) _{EC}	Stable	0.76	8.76	0.87	30.81	-2.54	958
			Unstable	0.84	-0.91	0.88	72.74	0.84	714
			All	0.81	8.41	0.96	52.95	0.88	1672
	(Rn-G) _{SRCas}	(H+LE) _{SRCas}	Stable	0.77	7.64	0.69	43.82	-2.10	959
			Unstable	0.91	9.50	0.84	64.12	0.94	709
			All	0.90	9.92	0.93	53.40	0.98	1668
	(Rn-G) _{SRShap}	(H+LE) _{SRShap}	Stable	1.04	-9.00	0.63	61.62	2.84	202
			Unstable	0.90	-1.80	0.50	123.21	0.90	196
			All	0.93	-10.17	0.80	96.97	0.87	398

10
11

1



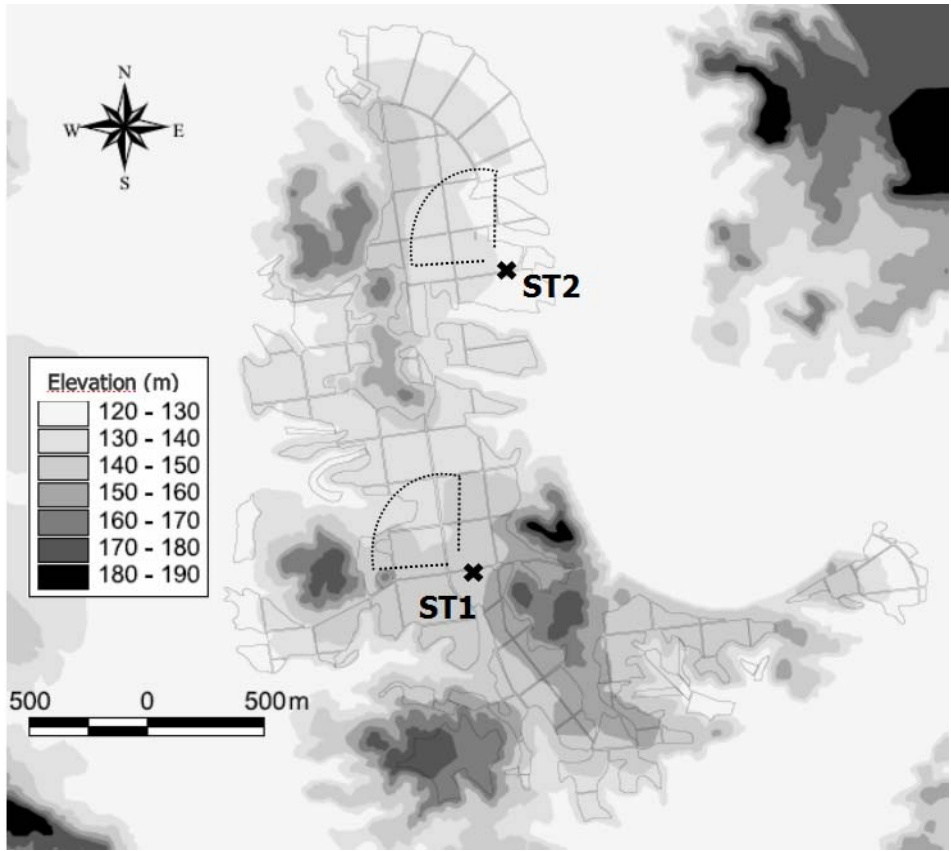
2



3

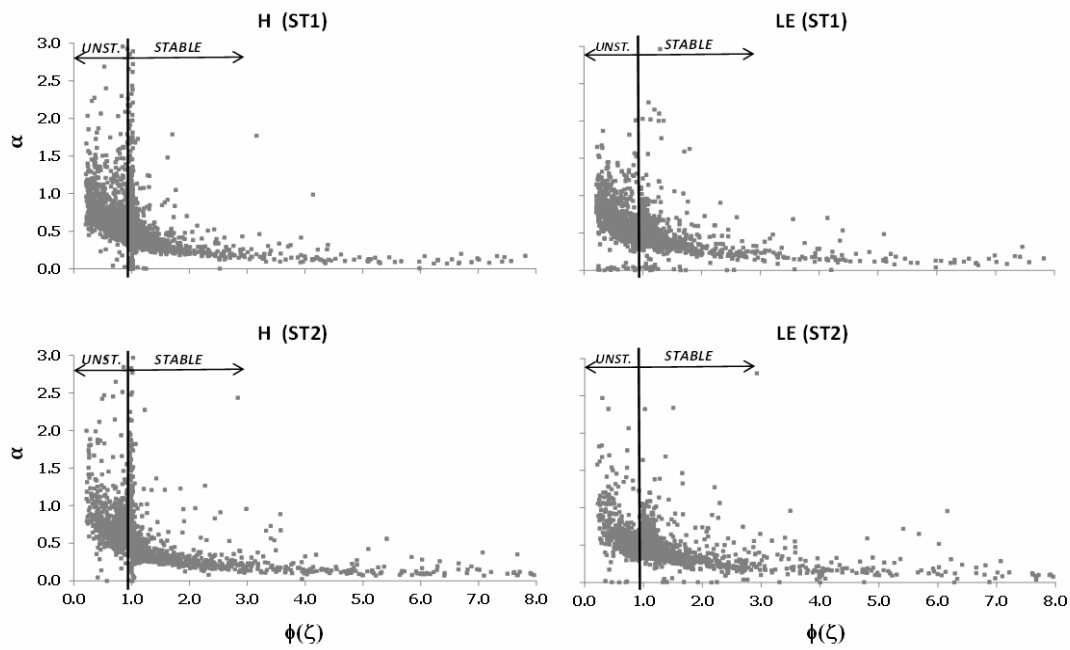
Figure 1. Location of the two micrometeorological stations at the commercial orchard La Herradura.

1
2



3
4
5
6
7

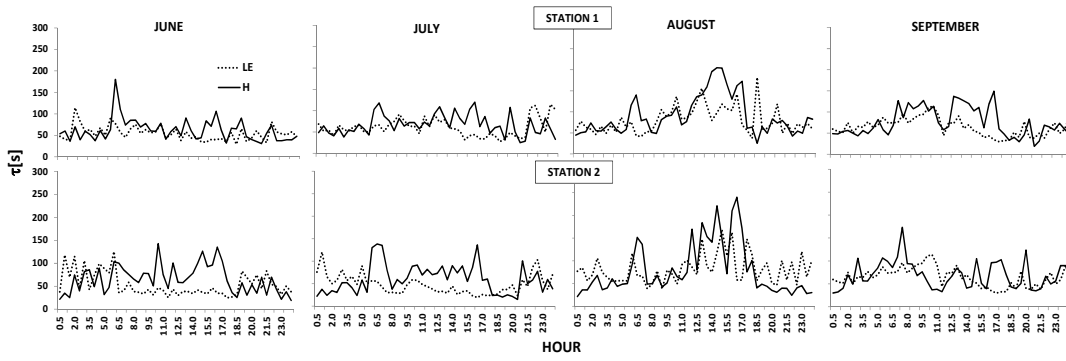
Figure 2. Topography of the study orchards and measurements' spots location. Dotted line are rough presentation of the footprint, with radius equal to minimum fetch requirement (377 m).



1

2 Figure 3. Surface renewal Castellvi approach (SR_{cas}) calibration factor (α) for both latent (LE) and
 3 sensible (H) heat flux estimation with respect to stability function ($\phi(\zeta)$). ST1, station located at late
 4 maturing peaches; ST2, station located at early maturing peaches.

1

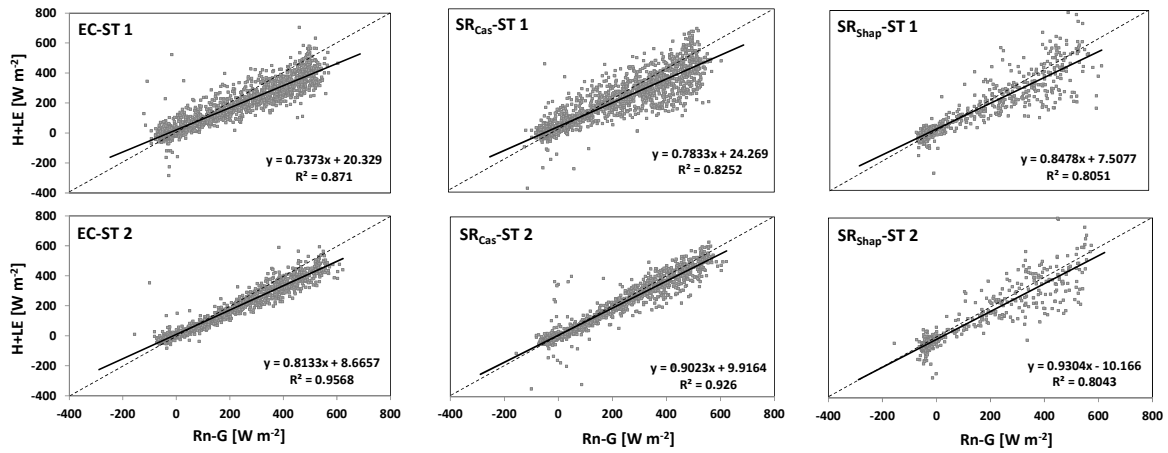


2

3

4 Figure 4. Monthly averages of the 30-min values of ramp duration (τ) for the sensible (solid line) and
5 latent (dotted line) heat fluxes obtained by the Surface renewal Castellvi approach (SR_{cas}) during the
6 4 months of the experimental measurement period. Station 1 at late peach spot; Station 2 at early
7 peach spot.

1



2

3 Figure 5. Measured available energy (net radiation minus soil heat flux, Rn-G) versus estimated scalar
4 fluxes (sensible and latent heat flux, LE+H) for both stations and methods used. ST1, late peaches;
5 ST2, early peaches; EC, eddy covariance; SR, surface renewal following the Castellví approach
6 (Castellvi, 2004; Castellvi et al., 2006, 2008). The data presented is for the whole measuring period
7 and all stability atmospheric conditions.

8